

# Deformation and dewetting of thin liquid films induced by moving gas jets

Christian W.J. Berendsen, Jos C.H. Zeegers, Anton A. Darhuber\*

Mesoscopic Transport Phenomena Group, Department of Applied Physics, Eindhoven University of Technology, Den Dolech 2, 5612AZ Eindhoven, The Netherlands

## ARTICLE INFO

### Article history:

Received 23 April 2013

Accepted 6 June 2013

Available online 26 June 2013

### Keywords:

Thin liquid films

Dewetting

Film rupture

Thin film instability

Impinging jets

## ABSTRACT

We study the deformation of thin liquid films subjected to impinging air-jets that are moving with respect to the substrate. The height profile and shape of the deformed liquid film is evaluated experimentally and numerically for different jet Reynolds numbers and translation speeds, for different liquids and substrate materials. Experiments and numerical results are in good agreement. On partially wetting substrates film rupture occurs. We imaged the appearance of dry spots and emergence of droplet patterns by high-speed, dual-wavelength interference microscopy. We systematically evaluated the resulting average droplet size and droplet density as a function of the experimental conditions. We show that within experimental accuracy the distribution of dry spots is dependent only on the residual film thickness and is not directly influenced by the shear stress and pressure gradients of the air-jet, nor by the speed of the substrate.

© 2013 Elsevier Inc. All rights reserved.

## 1. Introduction

The interaction between gas jets and moving liquid films is an important aspect of many technological processes. In the galvanization of steel, for example, so-called jet stripping is a common technique [1–8], where the thickness and uniformity of a metallic coating on a moving sheet of steel is adjusted by the pressure and shear stress of an impinging slot jet. The analogous effect is also relevant in smaller scale systems, such as ultrathin films of hard disk lubricant [9]. Moreover, gas jets were employed to study the influence of surfactants on the propagation of surface waves in a liquid film on a rotating disk [10].

When an impinging jet deforms a liquid film on a partially wetting substrate, the film can rupture [11–13] and start to dewet. Consequently air-jets are employed to initiate the redistribution of liquid in continuous coating of chemically patterned surfaces [14]. In immersion lithography [15–17], a photoresist covered silicon wafer is exposed through a layer of water in order to increase the effective numerical aperture of the illumination system. Controlled air-flows are utilized to contain the water meniscus between the objective lens and a partially wetting wafer, which is moving at a relative speed of approximately 1 m/s. Above a critical translation speed, however, a thin liquid film is left on the wafer, that spontaneously breaks up, dewets and leads to undesirable residual droplets on the substrate. Similar film rupture and dewetting phenomena have been described for thin layers of polymer melts [18–27], metals [28–32] and oil films submersed in water [33–35].

In this paper, we present a systematic study of the deformation of a moving liquid film due to laminar air-jets emanating from a round nozzle. We studied the behavior of four different liquids on both wetting and partially wetting substrates. We performed quantitative experiments and numerical simulations elucidating the dependence of the shape and minimum thickness of the deformed film on the operating parameters. The results were rationalized by means of a scaling analysis in the limit of high jet Reynolds numbers. On partially wetting substrates, we identified the minimum film thickness to be the crucial parameter governing the breakup process. We systematically varied the substrate speed and jet Reynolds number and determined the densities of dry-spots and residual droplets as well as the droplet size distribution. Using a geometrical scaling analysis [20], we derived power law relations for the droplet density and average droplet radius. Depending on the ratio of the dominant instability wavelength and the transverse lengthscale of the film deformation, a transition from two-dimensional to quasi-one-dimensional rupture patterns was observed.

## 2. Experiments

Fig. 1 shows a schematic representation of the experimental setup. A thin liquid film of initial thickness  $h_0$  on a transparent substrate is translated with respect to an air-jet that impinges at normal incidence. The air-jet is generated by maintaining an air flow  $Q_{\text{air}}$  through a round, hollow needle of inner diameter  $D$ . Its orifice is positioned at a distance  $H$  above the thin liquid film. A local depression, which we call *track*, is formed in the liquid film along the jet trajectory as shown in Fig. 2a. The liquid displaced from

\* Corresponding author.

E-mail address: a.a.darhuber@tue.nl (A.A. Darhuber).

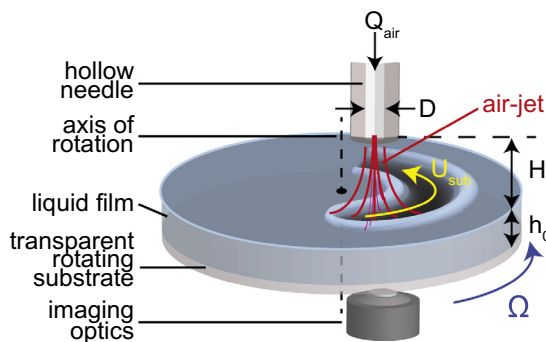


**Fig. 1.** Schematic of the experimental setup for measuring thin liquid film deformations by a moving air-jet. A circular air-jet is positioned at a distance  $H$  over a rotating sample coated with a liquid film of initial thickness  $h_0$ . The deformation of the film due to the impinging air-jet is imaged using interference microscopy with two alternating wavelengths of light.

the centerline of the jet trajectory is accumulated in a rim ahead and sideways of the jet impingement point. The yellow dashed line in Fig. 2a connects the local maxima of radial cross-sections of the rim. The maximum lateral extension of the rim is termed the track width  $w_{\max}$ . The distance between the jet stagnation point and the apex of the front rim is called  $a_{\text{front}}$ .

For the preparation of the thin liquid film and translation of the sample with respect to the impinging jet, we used a custom-designed spin-coater, where the sample and the area around the axis of rotation is optically accessible from both sides. Our spin-unit consists of a rotating sample holder that is supported by a hollow cylindrical roller bearing and driven by a tooth belt and a precision motor. Rotation speeds range between 0 and 6000 rpm with a resolution of 0.2 rpm. Transparent substrates were attached to the rotation stage using double-sided adhesive tape at the corners (3M Scotch 4016-1/2). As wetting substrates we used microscope cover glasses (Gold Seal,  $48 \times 60$  mm, Cat#63774-01), cleaned and rendered fully wettable by UV ozone treatment (Jelight) for 20 min. Partially wetting substrates were optical-quality polycarbonate film (PC, thickness  $750 \mu\text{m}$ , cut to the dimensions of

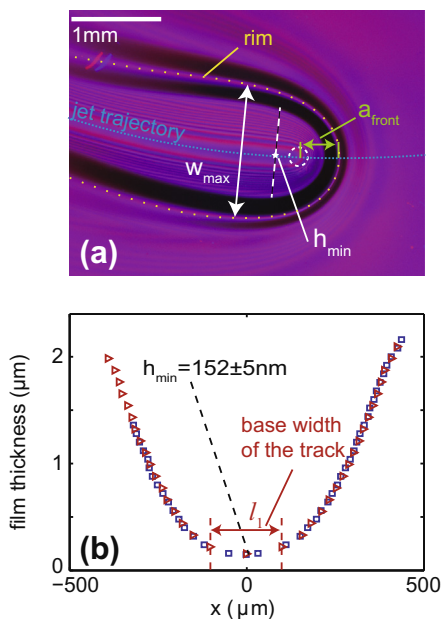


**Fig. 2.** (a) Typical example of a measurement, obtained with a substrate velocity  $U_{\text{sub}} = 2$  mm/s,  $Re_D = 346$  and needle diameter  $D = 208 \mu\text{m}$ . The image is an overlay of two consecutive interference patterns recorded at two different wavelengths. (b) Example of a height profile corresponding to the cross-section indicated by the dashed line in (a).

$60 \times 60$  mm), which we used as received after removal of the electrostatically bound protection foil. The non-zero conductivity of the liquid ensured that any residual static electricity was dissipated when the liquid was dispensed prior to spin coating.

Liquids used in this study were glycerol (Fluka, product number 49770, purity  $\geq 99.5\%$ ), triethylene glycol (3EG, Sigma, product number 95126, purity  $\geq 99\%$ ), ethylene glycol (1EG, J.T. Baker, product number 8201, MOS grade) and deionized water (Smart2-Pure, TKA, resistivity  $18.2 \text{ M}\Omega \times \text{cm}$ ). Table 1 presents viscosity  $\mu$ , surface tension  $\gamma$ , the typical refractive index for visible wavelengths  $n$  and the dielectric constant  $\epsilon_r$  for these liquids and their contact angles on polycarbonate. Advancing and receding contact angles on PC were measured by slowly increasing and decreasing the volume of a liquid droplet and capturing sideview images using a CMOS camera (Thorlabs DCC1645C) and telecentric lens (Moritex MML2-ST65). Unless specified otherwise, the experimental initial film thickness has the value listed in Table 1.

After spin coating, the rotating sample stage was decelerated to the rotation speed required for the impinging jet experiment. The air-jet was generated using a stainless steel hollow needle with inner diameter  $D = 208 \mu\text{m}$  and turned on by switching a two-way solenoid valve after reaching the required sample rotation speed. The needle was positioned at a distance  $H$  above the air-liquid interface at a radial distance of approximately 1 cm from the rotation center of the sample stage. The air (Linde,  $\text{N}_2/\text{O}_2$ -mixture, humidity  $< 200$  vpm, oil-free) was supplied from a gas cylinder through a precision pressure regulator (Norgren 11-818) and filters (Headline, 25-64-50C, 99.99% removal of  $0.1 \mu\text{m}$  particles and aerosols) before being admitted to a needle valve (Brooks NRS8514) that controlled the flow rate. The mass flow was measured using a mass flow meter (Bronkhorst F-201CV-2k).

The time evolution of the height profile of the liquid film was measured through the substrate by interference microscopy using two different wavelengths. The light source consists of two high-power light-emitting diodes (LED, Luxeon I) with center wavelengths of 466 nm and 655 nm and full width half maximum (FWHM) values of the light output spectrum of 28 nm and 22 nm, respectively. The LEDs were powered by two DC power supplies (Delta Electronics, ES030-5), collimated and combined using a 50:50 beamsplitter. The light sources were modulated in synchronization to the framerate of the camera, such that the illumination wavelength was alternating from frame to frame. For low-speed imaging at a framerate of 17 frames per second (fps), we used an InfiniTube lens system with a microscope objective (Mitutoyo, MPlan APO  $2\times/\text{NA} = 0.055$ ) and a CCD camera (Guppy, Allied Vision Technologies) and synchronized the light sources using Labview software and a data acquisition unit (National Instruments USB-6008). For imaging at 250 fps, we used a high-speed camera (Photron SA-4) fitted with a lens system and a microscope objective (Olympus, UPlan  $4\times/\text{NA} = 0.13$ ) in combination with a dual-channel function generator (Yokogawa FG120) to synchronize the light sources. The deformed height profile of the liquid film was determined from the position and number of the interference fringes, whereby the fringe order was established by a comparison of the interference patterns of both wavelengths. The minimum film thickness near the center of the jet impingement zone was estimated by grayscale interpolation for both wavelengths. For the material systems used, the accuracy of this method is typically better than 10 nm.

Fig. 2 illustrates the dual-wavelength interference technique for a typical experiment. In Fig. 2 the blue<sup>1</sup> and red interference micrographs are overlaid. In this particular example, a dust fiber on the

<sup>1</sup> For interpretation of color in Figs. 2 and 11, the reader is referred to the web version of this article.

Download English Version:

<https://daneshyari.com/en/article/6999493>

Download Persian Version:

<https://daneshyari.com/article/6999493>

[Daneshyari.com](https://daneshyari.com)